

Differential dynamics and stability of lamin A rod domain mutants

Kaushlendra Tripathi, Bhattiprolu Muralikrishna, Veena K Parnaik *

Centre for Cellular and Molecular Biology, CSIR, Hyderabad, India

Submitted: 6 Nov. 2008; Accepted: 30 Dec. 2008

Abstract

Mutations in the human lamin A gene give rise to highly debilitating diseases termed laminopathies. Laminopathic cells harboring certain mutations in lamin A display aberrant nuclear morphology due to abnormal lamina assembly. To understand the molecular mechanisms involved in these processes, we have studied the dynamics and stability of GFP-tagged lamin A constructs harboring disease-causing missense mutations in the rod and tail domains of the protein. Analysis of the mobilities of these proteins by fluorescence recovery after photobleaching (FRAP) and fluorescence loss in intensity after photobleaching (FLIP) techniques in live HeLa cells indicated that mutants that formed large aggregates, like E203G, G232E, Q294P and R386K were substantially more mobile than wild-type and mutant lamins H222P and R482L that assembled at the nuclear periphery. Nuclear extractions with detergent, nucleases and salt resulted in the dispersal of large aggregates into smaller foci throughout the nucleoplasm, whereas more stable lamins were retained at the nuclear periphery. The significant alterations in the dynamics and stability of certain rod domain mutants of lamin A are likely to have profound consequences for the organization of nuclear functions.

Keywords: lamin A; laminopathies; FRAP analysis; lamin A mutants; nuclear extraction.

INTRODUCTION

Lamins are the major constituents of a filamentous network of proteins that underlies the inner nuclear membrane and is termed the nuclear lamina. There are two classes of lamins: the B-type lamins that are expressed in all nucleated cells and the A-type lamins that have been detected primarily in differentiated cells. Two separate genes code for lamins B1 and B2, whereas the lamin A gene codes for the alternatively spliced products lamins A and C (termed lamin A/C). Lamins are involved in the organization of nuclear processes such as DNA replication and transcription, and also play a role in cellular signaling pathways. Mutations in the human lamin A gene (*LMNA*) cause a number of highly degenerative diseases collectively termed laminopathies that affect muscle, adipose, bone and neuronal tissues, and also cause premature ageing diseases (Worman and Courvalin, 2005; Broers *et al.*, 2006; Capell and Collins, 2006; Dechat *et al.*, 2008; Parnaik, 2008).

Lamins belong to the intermediate filament super family of proteins and possess a characteristic domain structure comprised of a short N-terminus followed by an α -helical rod domain and a globular C-terminal region that harbors an immunoglobulin-like (Ig) fold (Herrmann *et al.*, 2007). Two lamin monomers dimerise via coiled-coil interactions in the rod domain. Lamin filaments are formed by associations between protofilaments composed of lamin dimers. The Ig fold mediates interactions with various binding proteins. The stability of the lamina at the nuclear periphery has been well documented (Broers *et al.*, 1999; Moir *et al.*, 2000) and the effects of certain mutations on the stability of the peripheral lamina have been reported (Gilchrist *et al.*, 2004; Broers *et al.*, 2005; Wiesel *et al.*, 2008). However, there is limited information on the dynamics of lamin A mutants that form large intranuclear aggregates and cause aberrant nuclear morphology that is a hallmark of laminopathic cells.

In this report, we have compared the dynamics of lamin A mutants that predominantly form intranuclear aggregates with those that assemble at the nuclear rim by the techniques of fluorescence recovery after photobleaching (FRAP) and fluorescence loss in intensity after photobleaching (FLIP). Our data indicates that the mobilities of lamin aggregates are several-fold higher than those of lamins at the nuclear periphery in live HeLa cells. Further, these

*Corresponding author:
 Veena K Parnaik, Ph.D.
 Centre for Cellular and Molecular Biology
 Uppal Road,
 Hyderabad – 500 007, India
 Email: veenap@cmb.res.in

characteristics correlate well with the dispersal properties of the lamin mutants after nuclear extractions.

MATERIALS AND METHODS

Plasmid constructs

The cloning of wild-type GFP-lamin A and lamin mutant constructs has been described earlier (Mariappan *et al.*, 2005; Manju *et al.*, 2006).

Cell culture, DNA transfection and nuclear extractions

HeLa cells were routinely grown in DMEM supplemented with 10% FBS at 37°C in a humidified atmosphere containing 5% CO₂. Plasmid constructs were transiently transfected into HeLa cells for 24 h using Lipofectamine according to the manufacturer's instructions (Invitrogen, Carlsbad, USA). HeLa cell nuclei were extracted by a modification of the protocol of Nickerson *et al.*, (1992) as described earlier (Jagatheesan *et al.*, 1999). Briefly, cells grown on coverslips were washed in ice-cold cytoskeleton buffer containing 10 mM Pipes pH 6.8, 10 mM KCl, 300 mM sucrose, 3 mM MgCl₂, 1 mM EDTA, 0.05 mM phenylmethylsulphonyl fluoride (PMSF) and 10 µg/ml aprotinin. The cells were then incubated in cytoskeleton buffer containing 0.5% (v/v) Triton X-100 for 10 min at 4°C and rinsed in ice-cold RSB buffer (42.5 mM Tris.HCl pH 8.3, 8.5 mM NaCl, 2.6 mM MgCl₂, 0.05 mM PMSF and 10 µg/ml aprotinin). This was followed by incubation in RSB buffer containing 1% (v/v) Tween 20 and 0.5% (v/v) sodium deoxycholate for 10 min at 4°C. The cells were then rinsed in ice-cold digestion buffer (10 mM Pipes pH 8.3, 50 mM NaCl, 300 mM sucrose, 3 mM MgCl₂, 1 mM EGTA, 0.05 mM PMSF and 10 µg/ml aprotinin) and incubated with 100 units/ml of DNase I in digestion buffer for 30 min at 30°C. To remove digested material, 1 M (NH₄)₂SO₄ was added to a final concentration of 0.25 M for 5 min at 4°C. The samples were further extracted with 2 M NaCl for 5 min at 4°C and then fixed and processed for immunofluorescence microscopy or analyzed by western blots. Samples were monitored for efficiency of extraction by checking for the absence of DNA staining with DAPI.

Immunofluorescence microscopy

Transfected HeLa cells were fixed, permeabilised and treated with 0.5% gelatin in PBS for 1 h followed by incubation with primary antibody to lamin B1 or lamin A/C (Santa Cruz Biotechnology, Santa Cruz, USA) for 2 h and then Cy3-conjugated secondary antibody for 1 h at room temperature. Samples were mounted in Vectashield (Vector Laboratories, Burlingame, USA)

containing 1 µg/ml DAPI. Fluorescence microscopy of fixed cells was performed on an LSM510 META confocal microscope (Carl Zeiss, Oberkochen, Germany). DAPI staining was routinely viewed in the transmission mode. Images were analyzed with LSM 510 META software and assembled using Photoshop 6.0.

Live cell microscopy

HeLa cells transiently expressing GFP-lamin A constructs were seeded on a LabTekII chamber slide and grown for 24 h. FRAP experiments were performed on an LSM510 META inverted confocal microscope with a 63x/1.4 NA planapochromat water objective lens, as described previously (Tripathi and Parnaik, 2008). A suitable region of interest (ROI) was bleached for 0.5 sec using the 488 nm laser line at 100% laser power, and a series of images were acquired at 10-sec intervals immediately after bleaching, each as a 3D z-plane stack. Image acquisition was at low laser power that did not significantly affect fluorescence intensity. Recovery of fluorescence was observed for 2-3 h. Because of focus drift due to the length of the FRAP analysis, the best z-plane image for the bleach ROI was selected from each time-point 3D stack. All intensities were background subtracted for calculation of FRAP curves, which represented an average of 10-12 individual cells bleached under identical conditions in at least three independent experiments. To normalize for loss of fluorescence signal due to the bleach pulse and potential artifactual bleaching of GFP during the imaging scans, recovery intensities were normalized to the total fluorescence signal at each time point. Cells exhibiting a loss of signal of more than 10% during the imaging phase were discarded for analysis. The relative fluorescence intensity (RFI) at each time point was calculated as described by Phair and Misteli (2000), using the equation $RFI = (I_t/T_t)/(I_0/T_0)$ where I_0 and I_t are the average intensity of the region of interest before and after bleach at time t , and T_0 and T_t are the total intensity in the nucleus before and after bleach at time t . Half-time of fluorescence recovery ($t_{1/2}$) was calculated as half the time required for complete recovery of fluorescence after bleach (Moir *et al.*, 2000). FLIP-FRAP analysis was carried out as described (Mattern *et al.*, 2004; Essers *et al.*, 2005). Non-linear curve fitting was carried out using Origin 7.0. In control experiments with formaldehyde-fixed cells, no recovery of fluorescence was observed.

Western blot analysis

Unextracted or extracted HeLa cells were harvested, lysed in Laemmli's sample buffer, boiled and electrophoresed through SDS-10% polyacrylamide gels. Gels were electroblotted onto PVDF membrane filters and blocked overnight in 5% BLOTTO in Tris-buffered saline containing 0.1% Tween-20. Filters were

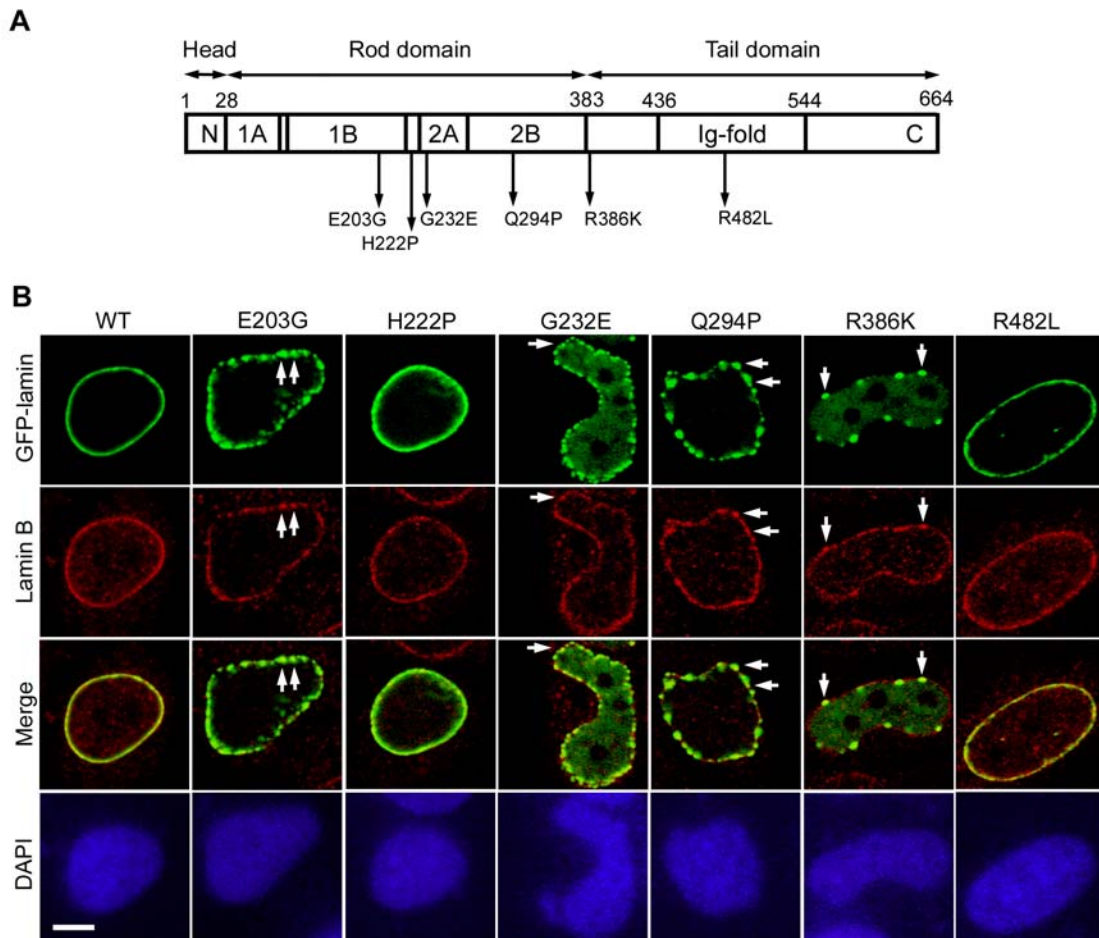


Figure 1: Assembly properties of GFP-tagged lamin constructs. (A) Domain structure of lamin A protein indicating disease-causing mutations that have been analyzed in this study. (B) Immunofluorescence analysis of GFP-tagged lamin constructs transiently transfected into HeLa cells and stained with anti-lamin B1 antibody and counterstained with DAPI. Arrows indicate discontinuous staining of lamin B1 aggregates and mutant GFP-lamins. Bar, 5 μ m.

incubated with primary antibody for 2 h, followed by alkaline phosphatase-conjugated secondary antibody for 1 h. The primary antibodies used were polyclonal antibodies to lamin A from Santa Cruz Biotechnology Inc., and to GFP from Abcam (Cambridge, UK). Bound antibody was visualized by a color reaction using nitroblue tetrazolium and 5-bromo-4-chloro-indolyl phosphate.

RESULTS

The lamin A mutations studied were E203G, H222P, G232E, Q294P, R386K, and R482L (see Fig. 1A for position of mutations). H222P, G232E, Q294P and R386K have been identified in autosomal dominant Emery-Dreifuss muscular dystrophy (AD-EDMD; Bonne *et al.*, 2000). E203G is mutated in dilated cardiomyopathy with conduction system disease (DCM; Fatkin *et al.*, 1999), and the R482L mutation is found in patients with familial partial lipodystrophy (FPLD; Shackleton *et al.*, 2000). E203G, H222P, G232E and

Q294P are present within the rod domain, R386K is located at the very C-terminus of the rod domain and R482L is in the globular tail domain. When GFP-tagged lamin constructs were expressed in HeLa cells, wild-type GFP-lamin A, H222P and R482L assembled at the nuclear rim in the majority of cells (~90%) while E203G, G232E, Q294P and R386K predominantly assembled into aggregates towards the periphery of the nucleus and also showed variable diffuse distribution in the interior, as observed earlier (Manju *et al.*, 2006; Parnaik and Manju, 2006). The smooth nuclear rim staining of the endogenous lamina was not perturbed upon expression of wild-type GFP-lamin A, H222P or R482L, as determined by staining with an antibody to lamin B1. However, in cells expressing the other mutants, the staining of lamin B1 was discontinuous and small aggregates of lamin B1 that colocalized with aggregates of lamin A mutants were observed at the nuclear periphery (Fig. 1B), suggesting that aberrant expression of lamin A affects the assembly of lamin B1 also.

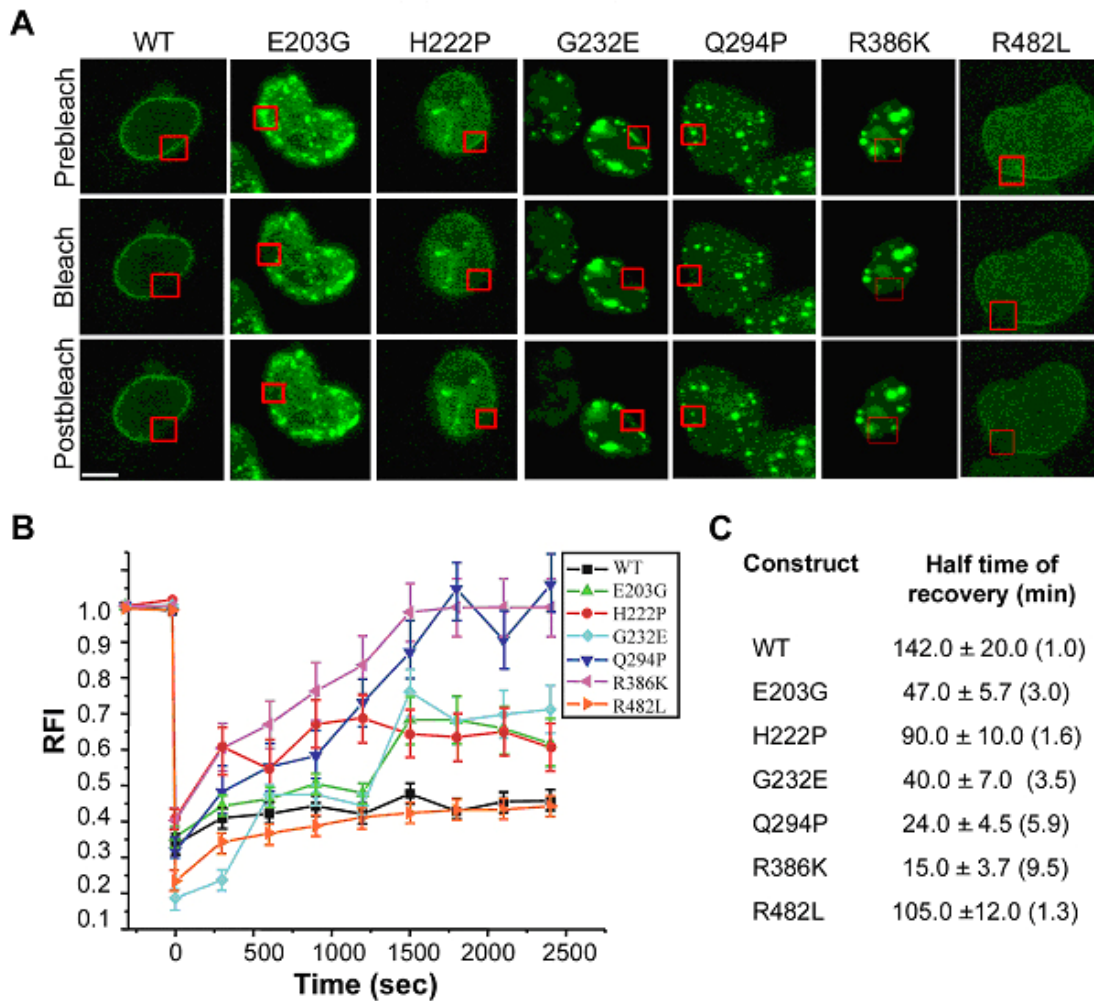


Figure 2: FRAP analysis of GFP-tagged lamin constructs. (A) Fluorescence images of FRAP processes of GFP-lamins for the indicated conditions. Rectangles indicate areas of bleaching where fluorescence recovery was measured. The illustrated postbleach time-point is 30 min after bleach. Bar, 5 μ m. (B) Graphical presentation of fluorescence recovery as change in relative fluorescence intensity (RFI) over time (postbleach as zero). Representative time-points are shown till 40 min postbleach. (C) Comparison of half time of recovery of different lamin mutants. Error bars represent \pm sd with $n=10$ to 12 individual cells. Numbers in brackets indicate fold decrease in comparison with wild-type.

Wild-type lamins fused to GFP form a stable polymer at the nuclear periphery with very slow dynamics and half time of recovery ($t_{1/2}$) of approximately 2h in photobleaching experiments (Broers *et al.*, 1999; Moir *et al.*, 2000). We investigated the dynamics of lamin mutants that predominantly form aggregates, such as E203G, G232E, Q294P and R386K, and compared the data with that of wild-type GFP-lamin A, H222P and R482L which assemble at the nuclear rim. FRAP experiments were carried out with HeLa cells transiently transfected with GFP-lamin A constructs. A suitable area was bleached and the recovery of fluorescence within the photobleached area was measured for 2-3 h. The fluorescence recovery curves were analyzed as described (Phair and Misteli, 2000; Moir *et al.*, 2000). Images of bleached cells and calculated $t_{1/2}$ values are shown in Fig. 2. The FRAP data indicated that the half-time recoveries of E203G,

G232E, Q294P and R386K were several-fold lower than wild-type lamin A, indicating substantially faster dynamics; furthermore, Q294P and R386K showed complete recovery after 30 min. The lamin mutants H222P and R482L showed slower dynamics, nearly comparable with wild-type GFP-lamin A, and this is consistent with their incorporation into a stable polymer at the nuclear periphery.

In order to further confirm that lamin mutants which form aggregates or are diffusely distributed are more mobile than wild-type lamin A, events occurring in a larger area were monitored by a combination of FLIP and FRAP analysis. For this analysis, half of the nucleus of the cell expressing the GFP-lamin A mutant was bleached by a single laser pulse and recovery was allowed to occur (see Fig. 3A for images). The quantitative analysis of the data was carried out as follows. FLIP was measured in the unbleached half of

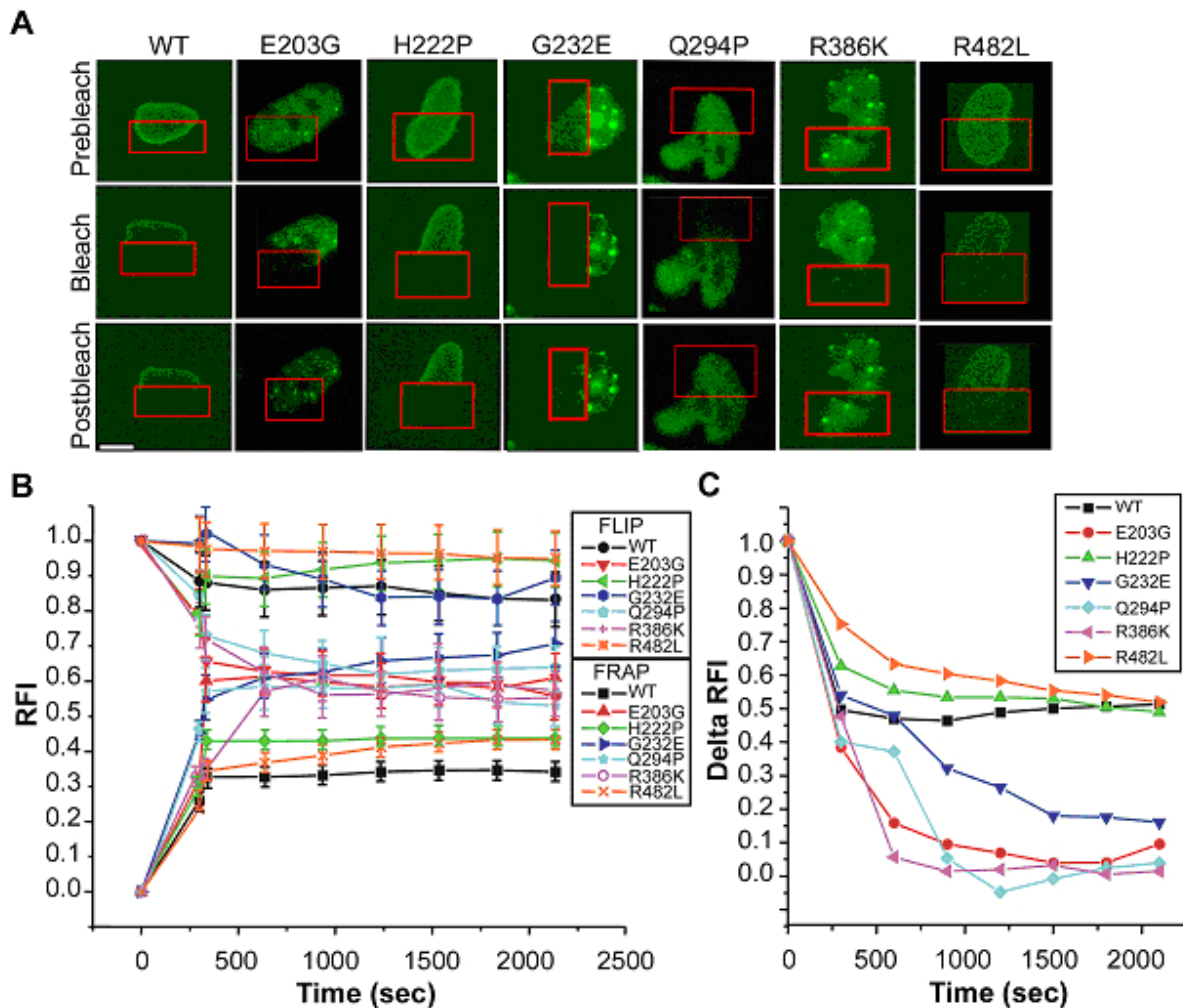


Figure 3: FLIP-FRAP analysis of GFP-tagged lamin constructs. (A) Fluorescence images of FLIP-FRAP processes of GFP-lamins. Rectangles indicate half of the nucleus where fluorescence recovery was measured; FLIP was calculated for the remaining half of the nucleus. The illustrated postbleach time-point is 30 min after bleach. Bar, 5 μ m. (B) Graphical presentation of fluorescence recovery or loss as change in relative fluorescence intensity (RFI) over time (postbleach as zero). Representative time-points are shown till 40 min postbleach. (C) Difference in fluorescence intensities between bleached and unbleached regions for various lamin mutants. Error bars represent \pm sd with $n = 10$ to 12 individual cells.

the nucleus while FRAP was measured in the bleached half of the nucleus. By this analysis, the fluorescence recovery in the boxed regions (which were photobleached) was simultaneously compared to the fluorescence loss in the remainder of the nucleus due to migration of fluorescent molecules into the bleached region, as reported for telomeric proteins (Mattern *et al.*, 2004) and proliferating cell nuclear antigen (Essers *et al.*, 2005). If the mutant is more mobile the FLIP and FRAP curves will converge, but will not converge if it is less mobile. Convergence of curves was observed with the mutants that formed aggregates or were diffusely distributed but not with those that assembled in a smooth rim at the periphery of the nucleus (Fig. 3B). The FLIP-FRAP data were also plotted as the difference in fluorescence intensities between bleached and unbleached regions. It was observed that E203G, G232E, Q294P and R386K took less time for recovery than R482L and H222P (Fig. 3C). These FLIP-FRAP

experiments clearly indicate that lamin mutants which form aggregates are more mobile.

The endogenous lamina is a very stable and insoluble structure that is resistant to extraction by detergents, nucleases and high salt. In order to determine the stability of the lamin assemblies formed by wild-type and mutant GFP-lamins, transfected cells were extracted as described in Materials and methods, and analyzed by fluorescence microscopy. The smooth peripheral location of endogenous lamins and wild-type GFP-lamin A was retained after nuclear extractions, as expected (Fig. 4A,B). The lamin mutants H222P and R482L were also mostly present at the nuclear rim. However, the localization of E203G, G232E, Q294P and R386K was significantly altered after extraction. Large peripheral aggregates were reduced in size and mutant lamins were distributed in small aggregates throughout the nucleus in the majority of extracted cells,

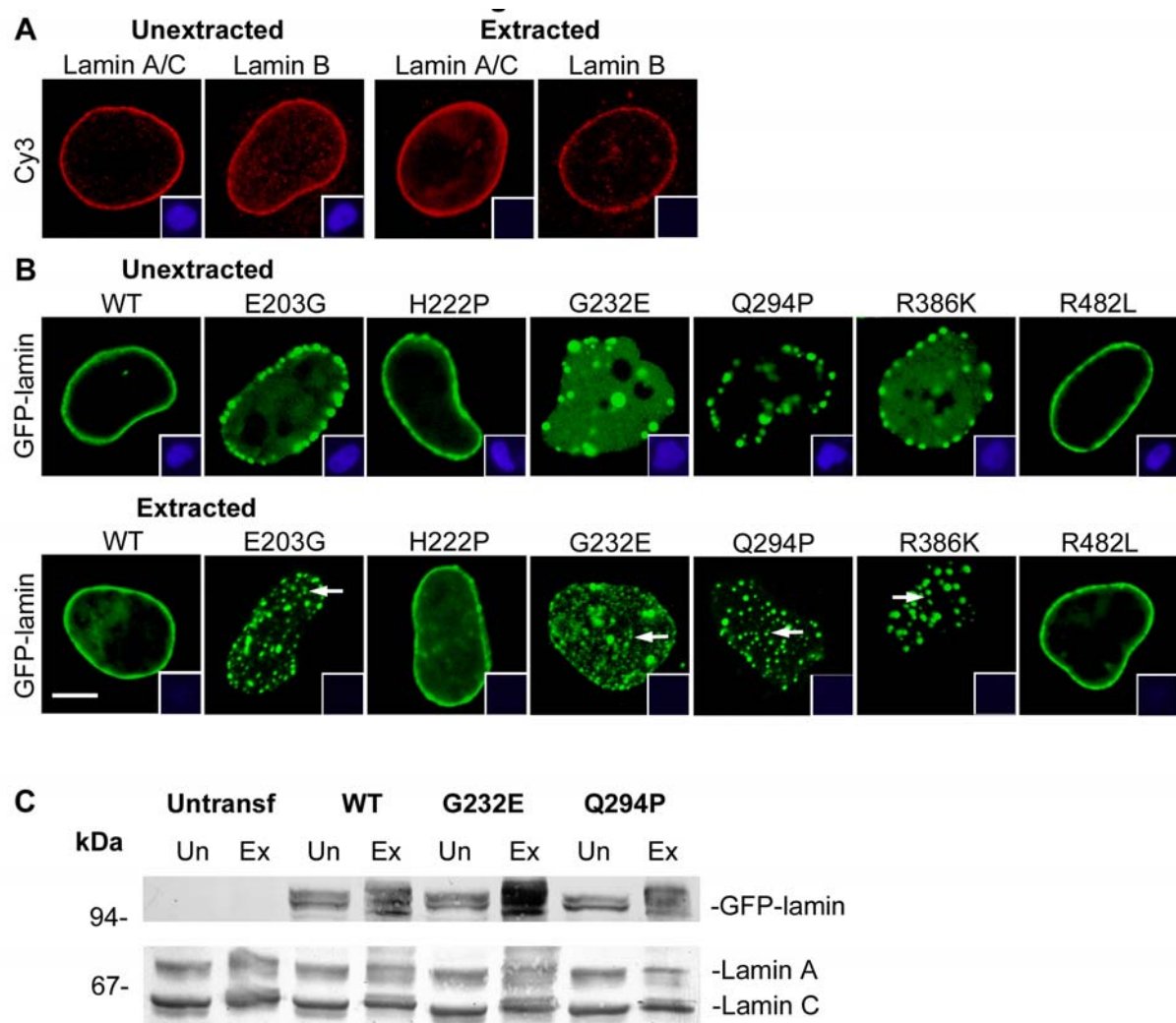


Figure 4: Assembly properties of GFP-tagged lamin constructs. (A) Immunofluorescence analysis of HeLa cells extracted with detergent, nucleases and salt and then stained with anti-lamin A/C or anti-lamin B1 antibody and counterstained with DAPI (insets). (B) Fluorescence analysis of extracted HeLa cells expressing GFP-tagged lamin constructs, counterstained with DAPI (insets). Arrows indicate nuclei displaying dispersed lamin foci. Unextracted cells are shown in both panels as controls. Bar, 5 μ m. (C) Western blot analysis of unextracted (Un) and extracted (Ex) HeLa cells expressing GFP-tagged lamin constructs and probed with antibodies to lamin A/C or GFP (both processed and unprocessed forms of GFP-lamins are detectable in lysates of wild-type and mutant constructs). Untransfected cells were also analyzed in the same blot.

suggesting that the mutant lamin assemblies were susceptible to the extraction conditions and thus less stable than the peripheral lamina. This is consistent with the faster mobility of these proteins in live cells. Although mutant lamins were redistributed after extraction, this treatment did not cause solubilization and subsequent depletion of the mutant proteins, as western blot analysis of representative constructs did not indicate a decrease in levels of GFP-lamins (Fig. 4C).

DISCUSSION

In this report, we have studied the dynamics and stability of lamin A and its disease-causing mutants in HeLa cells. Two distinct trends were observed for the

mobilities of lamin mutants from the FRAP and FLIP-FRAP analysis; lamin mutants that form large aggregates like E203G, G232E, Q294P and R386K were observed to be substantially more mobile when compared to wild-type and mutant lamins H222P and R482L which localize to the periphery of the nucleus. Upon nuclear extraction, large aggregates of lamin mutants were dispersed into smaller aggregates throughout the nucleus whereas more stable lamins were retained at the nuclear rim.

GFP-tagged wild-type lamin C, B1 and A exhibit very slow mobilities with half time recoveries of 2-3 hours, indicative of incorporation into a stable polymer at the nuclear periphery (Broers *et al.*, 1999; Moir *et al.*, 2000; Gilchrist *et al.*, 2004). On the other hand, half time recoveries of inner nuclear membrane proteins like

emerin, lamin B receptor and MAN1 are 1-2 minutes (Östlund *et al.*, 2006) and nucleoplasmic proteins such as the splicing factor SC35 show recoveries in the range of a few seconds (Phair and Misteli, 2000). The slow mobilities we have observed for H222P and R482L are consistent with their incorporation into a stable polymer at the nuclear periphery. As the R482 residue is exposed to the surface of the Ig-fold domain, a mutation at this site is unlikely to affect lamin polymerization (Dhe-Paganon *et al.*, 2002; Krimm *et al.*, 2002). Lamin A bearing another mutation at this site, R482W is also incorporated into a stable polymer (Raharjo *et al.*, 2001; Gilchrist *et al.*, 2004). The H222P mutation is located in the flexible linker region between coils 1B and 2A in the rod domain and this might explain why this construct shows a typical nuclear rim localization and slow dynamics. Furthermore, these properties are consistent with the milder properties of a knock-in-mouse model for EDMD with the H222P mutation (Arimura *et al.*, 2005). Another rod domain mutant, L85R is also localized at the nuclear rim and is only 2-fold more mobile than wild-type lamin A (Gilchrist *et al.*, 2004).

The faster mobilities observed for the lamin mutants E203G, G232E, Q294P and R386K are suggestive of unstable interactions between lamin molecules that lead to defects in assembly of stable polymers, as evident from formation of aggregates, disruption of the endogenous lamin network and depletion of the lamin-binding protein emerin from the nuclear envelope observed previously (Manju *et al.*, 2006). The amino acid residue affected in each mutation and its precise location in lower and higher order lamin structures are likely to affect the half lives of the lamin mutants to different extents. Molecular structures of small segments of coil 1A and 2B of the rod domain have been reported and mutations in coil 2B, including R386K have been proposed to affect higher order lamin assembly but not dimer formation (Strelkov *et al.*, 2004). In experimental systems, the R386K mutation strongly disrupts filament assembly; the R386K mutant is distributed in both aggregates and a diffuse nucleoplasmic location (Östlund *et al.*, 2001; Broers *et al.*, 2005; Manju *et al.*, 2006). FLIP studies with nucleoplasmic R386K suggest a 4.5-fold faster mobility than wild-type lamin A (Broers *et al.*, 2005). Another rod domain mutant, N195K is also distributed diffusely in the nucleoplasm and is 5-fold more mobile than wild-type lamin A (Gilchrist *et al.*, 2004). These mobilities for diffusely distributed mutants are in the range of mobilities we have observed for large aggregates, suggesting that both types of assemblies are inherently less stable due to defective filament assembly. The *C. elegans* homolog of the E203G mutation also impairs filament assembly (Wiesel *et al.*, 2008). However, as the rod domain mutations E203G, G232E and Q294P do not fall in the modeled regions, it is not possible to precisely define the molecular

interactions that may be affected by these mutations. Similarly, it is not clear why the rod domain mutations H222P or L85R do not affect filament assembly.

In addition to their typical localization at the nuclear periphery, lamins are also normally located in the interior of the nucleus in the form of foci or a diffuse network. Some of these intranuclear lamin structures have been implicated in establishing patterns of DNA replication sites and in organizing transcription (Dechat *et al.*, 2008; Parnaik, 2008). Interphase cells expressing GFP-tagged lamin A or B1 display uniform, diffuse nucleoplasmic fluorescence, which represents stable lamin-containing structures resistant to nuclear extraction (Moir *et al.*, 2000). A more dynamic internal lamin component that is susceptible to nuclear extraction is enriched in the G1 phase of the cell cycle (Broers *et al.*, 1999; Moir *et al.*, 2000; Muralikrishna *et al.*, 2004). The unusual extractibility of GFP-lamin A mutants that form large aggregates into dispersed small foci reflects two properties of these lamin assemblies. Firstly, these aggregates are unstable in contrast to the highly stable peripheral lamina that is not perturbed by nuclear extractions. Secondly, these nucleoplasmic aggregates are aberrant structures that are not part of the intranuclear diffuse lamin network that is susceptible to extraction.

In summary, our findings provide direct evidence for the inherent instability of lamin A mutants that form large intranuclear aggregates; this instability has not been observed in previous studies with lamins located at the nuclear rim. The dynamic properties of lamin mutants that are not properly assembled are likely to have deleterious consequences for nuclear organization and function; together with altered lamin-protein interactions or lamin modifications, these unstable structures are expected to contribute to disease manifestations.

Abbreviations

FRAP, fluorescence recovery after photobleaching; FLIP, fluorescence loss in intensity after photobleaching

Acknowledgement

We thank Nandini Rangaraj for expert assistance with confocal microscopy and FRAP experiments. Financial support of the Department of Biotechnology, India for this work is gratefully acknowledged. K. T. was supported by a pre-doctoral research fellowship from the Council of Scientific and Industrial Research, India.

References

- Arimura T, Helbling-Leclerc A *et al.* (2005) Mouse model carrying H222P-*Lmna* mutation develops muscular dystrophy and dilated cardiomyopathy similar to human striated muscle laminopathies. *Hum Mol. Genet.* **14**: 155-169.
- Bonne G, Mercuri E *et al.* (2000) Clinical and molecular genetic spectrum of autosomal dominant Emery-Dreifuss muscular dystrophy due to mutations of the lamin A/C gene. *Ann. Neurol.* **48**: 170-180.
- Broers JL, Machiels BM *et al.* (1999) Dynamics of the nuclear lamina as monitored by GFP-tagged A-type lamins. *J. Cell Sci.* **112**: 3463-3475.
- Broers JLV, Kuijpers HJH *et al.* (2005) Both lamin A and lamin C mutations cause lamina instability as well as loss of internal nuclear lamin organization. *Exp. Cell Res.* **304**: 582-592.
- Broers JL, Ramaekers FC *et al.* (2006) Nuclear lamins: laminopathies and their role in premature ageing. *Physiol. Rev.* **86**: 967-1008.
- Capell BC and Collins FS (2006) Human laminopathies: nuclei gone genetically awry. *Nat. Rev. Genet.* **7**: 940-952.
- Dechat T, Pflieger K *et al.* (2008) Nuclear lamins: major factors in the structural organization and function of the nucleus and chromatin. *Genes Dev.* **22**: 832-853.
- Dhe-Paganon S, Werner ED *et al.* (2002) Structure of the globular tail of nuclear lamin. *J. Biol. Chem.* **277**: 17381-17384.
- Essers J, Theil AF *et al.* (2005) Nuclear dynamics of PCNA in DNA replication and repair. *Mol. Cell. Biol.* **25**: 9350-9359.
- Fatkin D, MacRae C *et al.* (1999) Missense mutations in the rod domain of the lamin A/C gene as causes of dilated cardiomyopathy and conduction-system disease. *N. Engl. J. Med.* **341**: 1715-1724.
- Gilchrist S, Gilbert N *et al.* (2004) Altered protein dynamics of disease-associated lamin A mutants. *BMC Cell Biol.* **5**: 46.
- Herrmann H, Bar H *et al.* (2007) Intermediate filaments: from cell architecture to nanomechanics. *Nat. Rev. Mol. Cell Biol.* **8**: 562-573.
- Krimm I, Östlund C *et al.* (2002) The Ig-like structure of the C-terminal domain of A/C, mutated in muscular dystrophies, cardiomyopathy, and partial lipodystrophy. *Structure* **10**: 811-823.
- Jagatheesan G, Thanumalayan S *et al.* (1999) Colocalisation of intranuclear lamin foci with RNA splicing factors. *J. Cell Sci.* **112**: 4651-4661.
- Manju K, Muralikrishna Bh *et al.* (2006) Expression of disease-causing lamin mutants impairs the formation of DNA repair foci. *J. Cell Sci.* **119**: 2704-2714.
- Mariappan I and Parnaik VK (2005) Sequestration of pRb by cyclin D3 causes intranuclear reorganization of lamin A/C during muscle cell differentiation. *Mol. Biol. Cell* **16**: 1948-1960.
- Mattern KA, Swiggers SJJ (2004) Dynamics of protein binding to telomeres in living cells: Implications for telomere structure and function. *Mol. Cell. Biol.* **24**: 5587-5594.
- Moir RD, Yoon M *et al.* (2000) Nuclear lamins A and B1: Different pathways of assembly during nuclear envelope formation in living cells. *J. Cell Biol.* **151**: 1155-1168.
- Muralikrishna Bh, Thanumalayan S *et al.* (2004) Immunolocalization of detergent-susceptible nucleoplasmic lamin A/C foci by a novel monoclonal antibody. *J. Cell. Biochem.* **91**: 730-739.
- Nickerson JA, Krockmalnic G *et al.* (1992) A normally masked nuclear antigen that appears at mitosis on cytoskeleton filaments adjoining chromosomes, centrioles and midbodies. *J. Cell Biol.* **116**: 977-987.
- Östlund C, Bonne, G *et al.* (2001) Properties of lamin A mutants found in Emery-Dreifuss muscular dystrophy, cardiomyopathy and Dunnigan-type partial lipodystrophy. *J. Cell Sci.* **114**: 4435-4445.
- Östlund C, Sullivan T *et al.* (2006) Dependence of diffusional mobility of integral inner nuclear membrane proteins on A-type lamins. *Biochemistry* **45**: 1374-1382.
- Parnaik VK (2008) Role of nuclear lamins in nuclear organization, cellular signaling and inherited diseases. *Int. Rev. Cell Mol. Biol.* **266**: 157-206.
- Parnaik VK and Manju K (2006) Laminopathies: multiple disorders arising from defects in nuclear architecture. *J. Biosci.* **31**: 405-421.
- Phair RD and Misteli T (2000) High mobility of proteins in the mammalian cell nucleus. *Nature* **404**: 604-609.
- Raharjo WH, Enarson P *et al.* (2001) Nuclear envelope defects associated with *LMNA* mutations cause dilated cardiomyopathy and Emery-Dreifuss muscular dystrophy. *J. Cell Sci.* **114**: 4447-4457.
- Shackleton S, Lloyd DJ *et al.* (2000) *LMNA*, encoding lamin A/C is mutated in partial lipodystrophy. *Nat. Genet.* **24**: 153-156.
- Strelkov SV, Schumacher J *et al.* (2004) Crystal structure of the human lamin A coil 2B dimer: Implications for the head-to-tail association of nuclear lamins. *J. Mol. Biol.* **343**: 1067-1080.
- Tripathi T and Parnaik VK (2008) Differential dynamics of splicing factor SC35 during the cell cycle. *J. Biosci.* **33**: 345-354.
- Wiesel N, Mattout A *et al.* (2008) Laminopathic mutations interfere with the assembly, localization and dynamics of nuclear lamins. *Proc. Natl. Acad. Sci. USA* **105**: 180-185.
- Worman HJ and Courvalin J-C (2005) Nuclear envelope, nuclear lamina and inherited disease. *Int. Rev. Cytol.* **246**: 231-279.